ADVANCED FUNCTIONAL MATERIALS
www.afm-journal.de

The Role of Point Defects in Heterojunction Photocatalysts: Perspectives and Outlooks

Di Zu, Hehe Wei, Zezhou Lin, Xiaopeng Bai, Md Nahian Al Subri Ivan, Yuen Hong Tsang, and Haitao Huang**

The development of efficient photocatalysts is a mainstay for the advancement of photocatalytic technology. Heterojunction photocatalysts can overcome the inherent limitations of single photocatalysts, integrating the advantages of each component, and achieving efficient separation of photogenerated charges, making them a research focus in the field of photocatalysis. The role of point defects in photocatalytic reactions is diverse and can significantly influence the performance of photocatalysts. This review comprehensively summarizes the latest advancements in point defect engineering for the modulation of heterojunction photocatalysts. First, the types of point defects and their impact on photocatalytic processes are introduced. Subsequently, the common types of heterojunction photocatalysts are presented. Then, in accordance with recent research progress, the regulatory mechanisms of point defects within heterojunction photocatalysts are outlined, with a particular focus on their functions on surface/interfacial properties and photogenerated charge transfer processes. Finally, the challenges faced by point defect engineering in optimizing heterojunction photocatalysts and promising solutions are proposed. This review provides an in-depth understanding of the role of point defect engineering in heterojunction photocatalysts, with the expectation of offering insights into the development of highly active photocatalytic materials.

1. Introduction

Photocatalysis is a technology of harnessing inexhaustible solar energy, and converting it into chemical energy through the interaction between solar energy and photocatalysts.[1] It has the advantages of cost-effectiveness, environmental friendliness, mild reaction conditions, and no secondary pollution.[2] Moreover, photocatalysis has a very wide field of applications that includes environmental purification,[3] industrial raw material synthesis,[4] H_2 production,[5] CO_2 reduction,[6] organic synthesis,[7] and pollutant degradation,[8] etc. Despite these advantages of photocatalytic reactions, due to the intrinsic limitations of photocatalyst band structure and rapid recombination of photogenerated carriers,[9] the photocatalytic efficiency is still very low, which is a bottleneck for their further developments and industrial applications.[10] For instance, to achieve commercial applications, the solar-to-hydrogen conversion efficiency (STH) of photocatalytic water splitting should be higher than 10%. Nevertheless, most current photocatalytic systems struggle to attain this efficiency level.[11]

The selection of photocatalysts should meet both thermodynamic as well as kinetic requirements of photocatalytic reactions. Thermodynamically, photogenerated carriers should have sufficient redox capacity to participate in the surface reaction;[12] kinetically, effective separation and migration of photogenerated electron-hole pairs should be realized to improve photocatalytic activity.[13] A single semiconductor photocatalyst is expected to possess a narrow bandgap to achieve a broader range of light absorption and enhance the utilization of solar energy. Paradoxically, a narrow bandgap reduces the redox capacity of photogenerated electrons and holes, which makes the photocatalytic reactions unfavorable.[14]

Heterojunction photocatalysts can be used to break the limitation of the inherent band structure of a single semiconductor.[15] Heterojunction photocatalysts composite multiple materials together, which can not only break the thermodynamic and kinetic limitations of single photocatalysts but also realize efficient photogenerated charge separation.[16] This represents a pivotal direction in the current development of photocatalysts. In addition, the construction of heterojunctions also meets

D. Zu, Z. Lin, M. N. A. S. Ivan, Y. H. Tsang, H. Huang
Department of Applied Physics
The Hong Kong Polytechnic University
Hung Hom, Kowloon, Hong Kong 999077, China
E-mail: yuen.tsang@polyu.edu.hk; aphhuang@polyu.edu.hk

H. Wei
State Key Laboratory of Green Chemical Engineering and Industrial Catalysis
Center for Computational Chemistry and Research Institute of Industrial Catalysis
School of Chemistry and Molecular Engineering
East China University of Science and Technology
130 Meilong Road, Shanghai 200237, China

X. Bai
Department of Mechanical Engineering
The University of Hong Kong
Hong Kong 999077, China

The ORCID identification number(s) for the author(s) of this article can be found under https://doi.org/10.1002/adfm.202408213

DOI: 10.1002/adfm.202408213

the performance requirements for applications in the field of photoelectrocatalysis.[17]

In order to enhance photocatalytic efficiency, numerous strategies have been developed to modify photocatalysts. Among them, point defect engineering stands out as an effective modulation strategy.[18] The second law of thermodynamics indicates that point defects in crystalline materials are indispensable. Historically, point defects are called "centers," such as color centers or F-centers in luminescent materials. Nowadays, the engineering of point defects has evolved from early-stage fundamental research to a modern technique widely used in the field of photocatalysis for the tuning of electronic structures of photocatalysts. Point defects induce imperfections in the lattice structure, adjusting the surface morphology along with electronic structure,[19] and further optimizing the physical as well as chemical properties of materials.[20] The alteration of geometrical structure and electronic arrangement by point defects can change the surface structure,[21] energy band arrangement,[22] charge separation transfer kinetics,[23] surface adsorption, and other properties related to photocatalysts,[24] which positively affect the photocatalytic process and significantly enhance the photocatalytic efficiency.

Considering the potential that point defect engineering has demonstrated in the field of photocatalysis, introducing it into highly promising heterojunction photocatalysts is a significant research idea to guide the development of highly active photocatalysts. However, till now there has been a lack of systematic compilation and summarization of research work in this area. For example, the role of point defects in the thermodynamic and kinetic processes of the reaction when they exist in heterojunction photocatalysts, the effect of point defects on key parameters such as band structure matching, interfacial characteristics, built-in electric fields, and charge transfer kinetics of heterojunctions, and the possibilities of triggering unique phenomena in photocatalytic reaction processes by the combination of point defects with heterojunctions are still not well summarized. Therefore, it is very important to generalize the regulation laws of point defects on the structure and performance of heterojunction photocatalysts for leading the design of efficient heterojunction photocatalysts.

In this review, first, the types of point defects, and their influence laws governing the photocatalytic reaction process are summarized; second, the classification of photocatalyst heterojunctions are discussed; third, the roles of point defects in heterojunction photocatalysts including their effects on band structure, interfacial contacts, built-in electric fields, charge transfers, redox reactions on the surfaces, etc. are discussed; and finally, the challenges and prospects of exploring point defects in heterojunction photocatalysts are put forward. This review aims to pave the way for employing point defects engineering to develop highly active photocatalysts and provide new ideas for solving the key problems in this field.

2. Basic Principles of Photocatalysis

As shown in **Figure 1**, semiconductor materials have a unique band structure, with the highest occupied molecular orbitals interacting to form the valence band (VB), the lowest unoccupied molecular orbitals interacting to form the conduction band (CB).

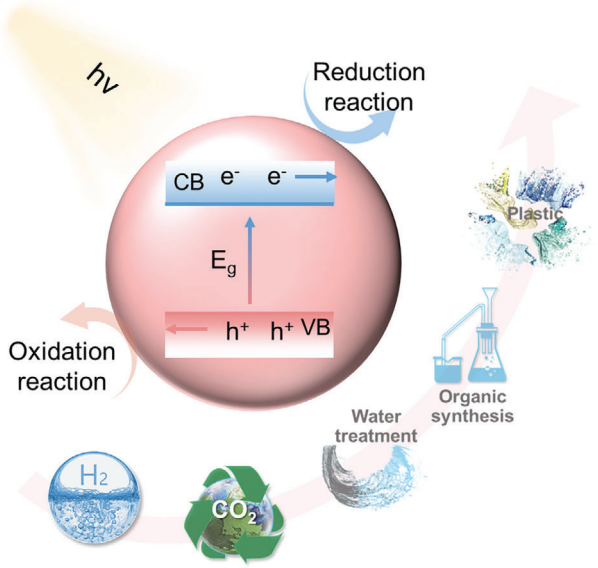

Figure 1. Schematic diagram for the photocatalytic process.

The intermediate region between the CB and VB known as the forbidden band, and the value of the forbidden band is denoted as E_g.[25] The reaction process of semiconductor photocatalysts is divided into three steps: 1) when the photocatalyst absorbs photons with energy (hν) greater than or equal to E_g, the electrons leap from VB to CB, which are known as photogenerated electrons, with the ability of reduction. Meanwhile, the holes left within VB are referred to as photogenerated holes, with the ability to oxidize. Photogenerated electrons and holes are also referred to as photogenerated carriers; 2) subsequently, the photogenerated electrons and holes migrate to the surface under the action of an electric field or by diffusion. During this process, a large number of photogenerated carriers recombine and the energy is released in the form of thermal or optical energy; and 3) finally, the photogenerated holes and electrons that migrate to the catalyst surface undergo oxidation and reduction reactions, respectively, with the surface adsorbed substances.[26]

The efficiencies of these three processes together determine the overall efficiency of photocatalysis,[27] which can be expressed by the following equation:

$$\eta_{tot} = \eta_{abs} \times \eta_{cs} \times \eta_{red} \quad (1)$$

η_{tot}: Total photocatalytic efficiency; η_{abs}: Light absorption efficiency; η_{cs}: Charge separation efficiency; η_{red}: Efficiency of surface redox chemical reactions.

The overall efficiency of the photocatalytic process remains low till now due to the limitations of the inherent properties of photocatalysts.

3. Types of Point Defects

Point defects refer to the local deviations from perfect periodicity in the arrangement of atoms within the lattice structure of crystalline materials. These deviations can be caused by the absence or replacement of individual or multiple atoms. They are small in

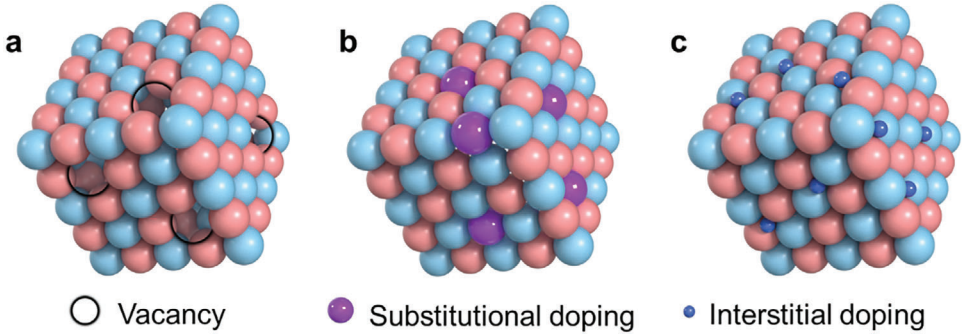

Figure 2. Schematic illustration of point defects. a) Vacancy. b) Substitutional doping (including antisite substitution). c) Interstitial doping.

all 3D scales and do not exceed a few atomic diameters.[28] Point defects are ubiquitous in semiconductors and can affect atomic arrangement and electronic bonding,[29] thereby regulating the optical,[30] electrical,[31] magnetic,[32] and thermal[33] properties of semiconductor materials.

Point defects can be categorized into two forms: vacancies and dopants.[34] Vacancies refer to the absence of original atoms or ions in the lattice, leaving empty sites (**Figure 2a**). This type of defect can create local disordered structures in the lattice, causing local charge imbalance in the crystal, and may change the valence state of ions adjacent to vacancy sites.[35] Doping foreign elements in the semiconductor host represent another significant type of point defect.[36] These dopant ions or atoms can be placed within the host lattice by replacing existing ions or atoms, known as substitutional doping (Figure 2b) or foreign elements can occupy interstitial positions in the lattice, defined as interstitial doping (Figure 2c). Substitutional doping may also include antisite substitution, where different atoms just exchange their atomic positions in an ordered compound. The introduction of doping often leads to lattice distortion and can regulate the composition of semiconductor photocatalysts.[37]

4. Effects of Point Defects on Photocatalytic Processes

4.1. Optical Absorption

The light absorption properties of semiconductors are directly related to their band alignment. However, for large bandgap semiconductors, their optical absorption is limited to the ultraviolet ($\lambda < 380$ nm) region, which accounts for only 7% of the energy of the entire solar spectrum.[38] Therefore, there is a need to explore ways to utilize light from the visible (50%) to the infrared (43%) regions, which account for the majority of the solar spectrum's energy.[39]

Point defects can alter the periodic potential field generated by the periodic arrangement of atoms, disrupting the original band structure by introducing new energy levels, which have a decisive influence on the properties of semiconductors.[40] This approach is widely utilized for adjusting the band alignment of a single semiconductor.[41]

The impurity energy levels introduced by point defects can be classified as acceptor levels and donor levels, which are typically located within the bandgap of the semiconductor.[42] Donor levels are situated close to the conduction band minimum (CBM), while acceptor levels are near the valence band maximum (VBM). Under the irradiation of photons with appropriate energy, the electrons and holes bound by the impurity levels can also undergo optical transitions. The absorption of photons can cause electrons at a neutral donor level to transit from the ground state to an excited state or to the CB, and holes at a neutral acceptor level can transit from the ground state to an excited state or to the VB.[43] Therefore, photon energy less than E_g can be absorbed by the impurity energy level, which broadens the range of light absorption.[44]

4.2. Photogenerated Charge Separation and Transfer

The kinetic process of charge separation and transfer in photocatalytic reactions is quite complex. Photogenerated charge separation and migration occur over a wide range of time periods (ps-μs), undergo multiple processes (such as relaxation, migration, diffusion, and defect state trapping), and are highly susceptible to recombination.[45] As a result, the photogenerated electrons and holes have very short lifetimes on the order of ps to ns, and the amount of photogenerated charges that can eventually transfer to the semiconductor surface to participate in chemical reactions is very limited, which is the biggest bottleneck that constraints the efficiency of photocatalytic reactions.[46]

Point defects play an important role in the photogenerated carrier separation process. The appropriate concentration and type of point defects add additional defect states inside the semiconductor energy bandgaps, and the defect states selectively trap the photogenerated carriers, providing additional paths for photogenerated charge transfer and facilitating space charge separation.[47] However, defect states sometimes become the recombination centers of photogenerated charge carriers, which reduces the charge separation efficiency and is detrimental to photocatalytic reactions.[48] Point defects also affect the charge transport properties, and the defect states can change the acceleration vector of free carriers and create potential barriers or energy channels.[49]

In addition to modulating the charge transfer path, point defects can also provide the driving force for charge separation. Photogenerated electrons and holes need to be separated from the interior of micro and nano-scale particles, where the required

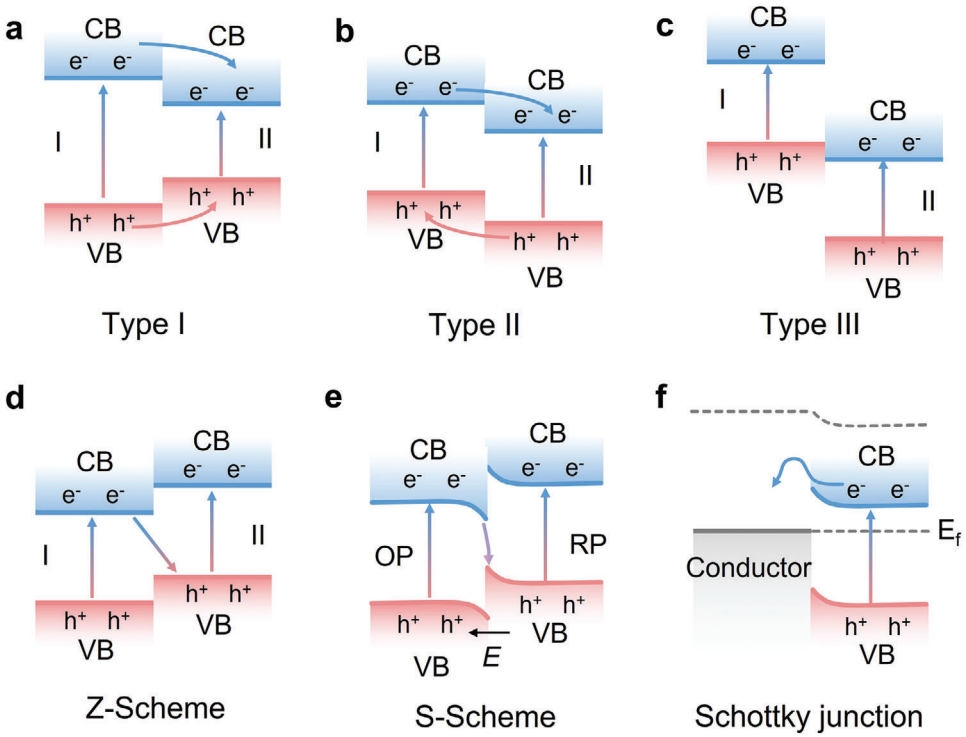

Figure 3. Schematic diagram for different types of heterojunction photocatalysts. a) Type I. b) Type II. c) Type III. d) Z-Scheme. e) S-Scheme. f) Schottky junction.

driving force is insufficient due to the small physical scale. Point defects can induce an imbalance in charge distribution, creating a built-in electric field that effectively promotes photogenerated charge separation.[50] Given the multiple roles of point defects and the complex charge separation process, it is essential to design point defects in a rational manner.

4.3. Surface Redox Reactions

Redox reactions occur on the surface of photocatalysts, involving the transfer of photogenerated charges at the adsorbed species/photocatalyst interface.[2a] High overpotentials and low kinetic rates are detrimental to the surface redox reactions and may increase the chance of surface charge recombination of photogenerated electron-hole pairs.[51]

From the thermodynamic perspective, point defects can modulate the positions of CBM and VBM. Accordingly, the redox capacity of photogenerated carriers reaching the surface of the photocatalyst can be altered, impacting the surface reaction. In terms of kinetics, point defects can regulate the active sites on the photocatalyst surface and the adsorption characteristics of the reacting molecules. The modulation of reaction kinetics by point defects can be classified into the following categories. i) Catalytic activity: The introduction of point defects generates thermodynamically unstable ligand-unsaturated metal atoms and surface dangling bonds. The ligand-unsaturated metal atoms can lead to local charge accumulation, which polarizes the adsorbed molecules, facilitating the activation of molecules.[12] ii) Surface charge transport: Point defects at the surface of photocatalysts can act as trapping centers for photogenerated carriers, providing charged sites to promote electrostatic adsorption of molecules and polarization of bonds,[52] and further affect the transfer of photogenerated electrons from semiconductor to surface-adsorbed molecules.[24] iii) Surface mass transport: Point defects can also alter the surface hydrophilicity of photocatalysts and affect the mass transport of reactants and reaction products.[53]

5. Types of Heterojunction Photocatalysts

In single photocatalysts, the overall energy conversion efficiency remains low due to poor light absorption, large recombination of photogenerated electrons and holes, and slow kinetics of the redox reaction process. Among them, achieving efficient photogenerated charge separation and transfer is the core challenge for photocatalysis.[23] Heterojunction structures are proven to be extremely efficient for the preparation of advanced photocatalysts due to their feasibility and effectiveness in spatial separation of the photogenerated electron-hole pairs.[54]

Heterojunction photocatalysts refer to the combination of two or more different photocatalysts, by which not only the separation of photogenerated carriers can be effectively enhanced, but also the redox ability of photogenerated charges can be fine-tuned. Typically, the following types of heterojunction photocatalysts exist: i) Type I, ii) Type II, iii) Type III, iv) Z-scheme, v) S-scheme and vi) Schottky junction, which are depicted in **Figure 3** and described in the following sections.

5.1. Type I

As shown in Figure 3a, in type I heterojunction, the bandgap of one semiconductor (semiconductor II in this case) is completely located within the forbidden band of the other semiconductor. Upon exposure to light, the photogenerated electrons will be transferred from CB of I to CB of II, driven by the potential difference, and at the same time the photogenerated holes will also be transferred from VB of I to VB of II. The photogenerated holes and electrons in semiconductor II will take part in the photocatalytic redox reaction.[55] Through this charge transfer method, the photogenerated charges may have a longer lifetime,[56] however, they are not spatially separated. Moreover, the photogenerated charge carriers that ultimately participate in the redox reaction have a lower potential, making the redox process thermodynamically unfavorable.

5.2. Type II

The CBM and VBM positions of the two semiconductors in Type II heterojunction are interleaved (Figure 3b). Under light excitation, the photogenerated electrons migrate from semiconductor I with a relatively higher CBM position to semiconductor II, while the photogenerated holes transfer from semiconductor II with a relatively lower VBM position to semiconductor I.[57] This charge transfer mechanism can effectively realize the spatial separation of photogenerated electron-hole pairs. However, similar to Type I heterojunction, this charge transfer mechanism imparts a lower redox potential to the photogenerated carriers involved in the reaction.

5.3. Type III

In Type III heterojunction photocatalysts, the difference in the band structure between the two semiconductors is extremely significant (Figure 3c), with no overlapped bandgaps of the two semiconductors.[58] Consequently, this distinctive feature impedes the effective separation and migration of photo-induced charge carriers at the interfacial region, rendering this type of heterojunction less attractive for photocatalytic applications. Hence, research in this area is relatively scarce. If an appropriate conductive medium can overcome the high energy barrier for charge transfer, allowing the photogenerated holes in VB of semiconductor I to combine with the photogenerated electrons in CB of II, there is the possibility to unlock the potential of Type III heterojunction.

5.4. Z-Scheme

Z-Scheme is one of the optimal heterojunction structures for enhancing photocatalytic activity, inspired by the electron transfer pathways in the natural photosynthesis system of green plants, following the shape of a "Z".[59] As shown in Figure 3d, an all-solid-state Z-Scheme system involves direct contact between two semiconductor photocatalysts (I and II) with staggered band structure.[60] Under illumination, the photogenerated electrons in CB of I will transfer to the interface and recombine with the holes in VB of II due to strong electrostatic attraction, thereby retaining electrons with stronger reducibility in CB of II and holes with stronger oxidizing power in VB of I.[61] The matched band structure and close contact (physical or chemical bonding) between the two semiconductors are crucial in this structure (sometimes with a redox mediator) to promote direct electron transfer and reduce the transfer distance of charge carriers.[62] Another all-solid-state Z-Scheme system involves the formation of an ohmic connection between I and II by a conductive medium, thereby reducing the resistance to charge separation and transfer.[63]

5.5. S-Scheme

S-Scheme (Step-Scheme) heterojunction is a refinement of the direct Z-Scheme and is a more accurate model of this type of heterojunction.[64] As depicted in Figure 3e, it consists of two semiconductors, oxidized photocatalyst (OP) with a more positive VBM and reduced photocatalyst (RP) with a more negative CBM. Upon contact, due to the difference in work function (WF), electrons are transferred from RP with lower WF to OP with higher WF. In this way, a built-in electric field is formed at the interface.[65] Upon light irradiation, through the synergistic effects of the built-in electric field, band bending, and electrostatic interactions, the photogenerated electrons at CB of OP merge with the photogenerated holes located at VB of RP, which promotes the separation of photogenerated carriers. Notably, photogenerated carriers with stronger redox capacity are retained and participate in the photocatalytic reaction.[66] In this way, S-Scheme photocatalysts can simultaneously achieve efficient space charge separation and high redox potentials for photogenerated carriers.

5.6. Schottky Junction

Schottky junction represents a heterojunction formed by a semiconductor and a conductor (Figure 3f). The difference in WF serves as a driving force for the interfacial charge exchange.[67] Taking the example of an n-type semiconductor-conductor Schottky junction, when the WF of the semiconductor is lower than that of the conductor, electrons migrate from the n-type semiconductor to the conductor until the Fermi levels (E_f) of both are aligned. Consequently, a space charge layer forms at the interface, resulting in the formation of a Schottky barrier between the conductor and the semiconductor. Under light excitation, photogenerated electrons in the semiconductor are transferred to the conductor, which is also known as an electron sink.[68] The establishment of the Schottky barrier facilitates the continuous migration of photogenerated electrons, enhances the separation of photogenerated charges, and is beneficial for the participation of holes in reactions, thereby improving photocatalytic activity.

6. Regulatory Mechanisms of Point Defects in Heterojunction Photocatalysts

Rationally constructed heterojunctions can overcome the limitations of single photocatalysts, broaden the light absorption

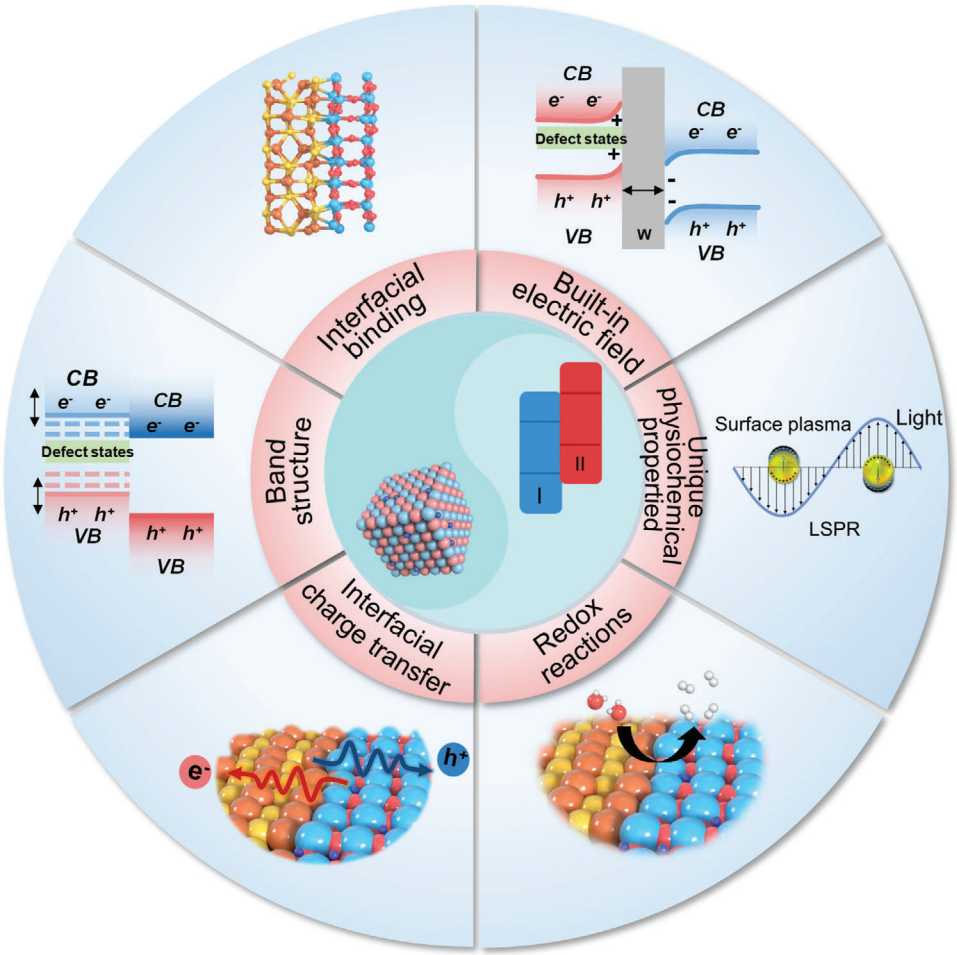

Figure 4. Schematic illustration of the role of point defects in heterojunction photocatalyst.

range, accelerate the effective separation of photogenerated carriers, and improve the photocatalytic reaction efficiency.[69] However, heterojunction photocatalysts face the limitations of unfavorable factors such as high interfacial energy barriers,[70] small range of action of the built-in electric field,[71] and insufficient exposure of active sites on the surface,[14] which impede their developments toward practical applications. Previous studies have incorporated point defects into heterojunctions to overcome the limitations of unfavorable factors and investigated the point defect modulation mechanisms. This section details the regulatory mechanisms of point defects for the key parameters of heterojunction materials (**Figure 4**), aiming to pave the way for the optimum design of point defect heterojunction photocatalysts.

6.1. Band Structure

The matching of band structure is a prerequisite for the construction of effective heterojunction photocatalysts.[72] The photocatalytic reaction has a certain requirement for the band structure of the material. According to the effect of point defects on the band structure of a single semiconductor, for heterojunction photocatalysts, the band structure can be regulated by modulating the type and concentration of point defects, which provides a flexible and controllable way to match the energy bands of the heterojunction.[73]

For example, Zhao et al. introduced both B dopant and N vacancy into 2D g-C_3N_4 nanosheets ($BDCNN_x$) using $NaBH_4$ thermal reduction.[74] The pristine 2D g-C_3N_4 nanosheets (CNN) is an H_2 evolution photocatalyst, and by tailoring the concentration of B dopants and N vacancies, the VBM and CBM of CNN can be tuned continuously, resulting in a series of H_2 and O_2 evolution photocatalysts (**Figure 5a**). The combination of the H_2 and O_2 evolution photocatalysts through electrostatic self-assembly results in large interfacial contact and efficient charge transfer (Figure 5b). Among these self-assembled heterostructures, $BDCNN_{350}/BDCNN_{425}$ exhibits the highest photocatalytic activity with the STH reaching 1.16% (Figure 5c). A series of experimental characterizations and theoretical calculations demonstrate that B dopant and N vacancy can modulate band structure, which endows the heterostructure with enough driving force for the water redox reactions and facilitates charge separation and transfer in a direct Z-scheme pathway, thereby (Figure 5d), resulting in excellent photocatalytic overall water splitting.

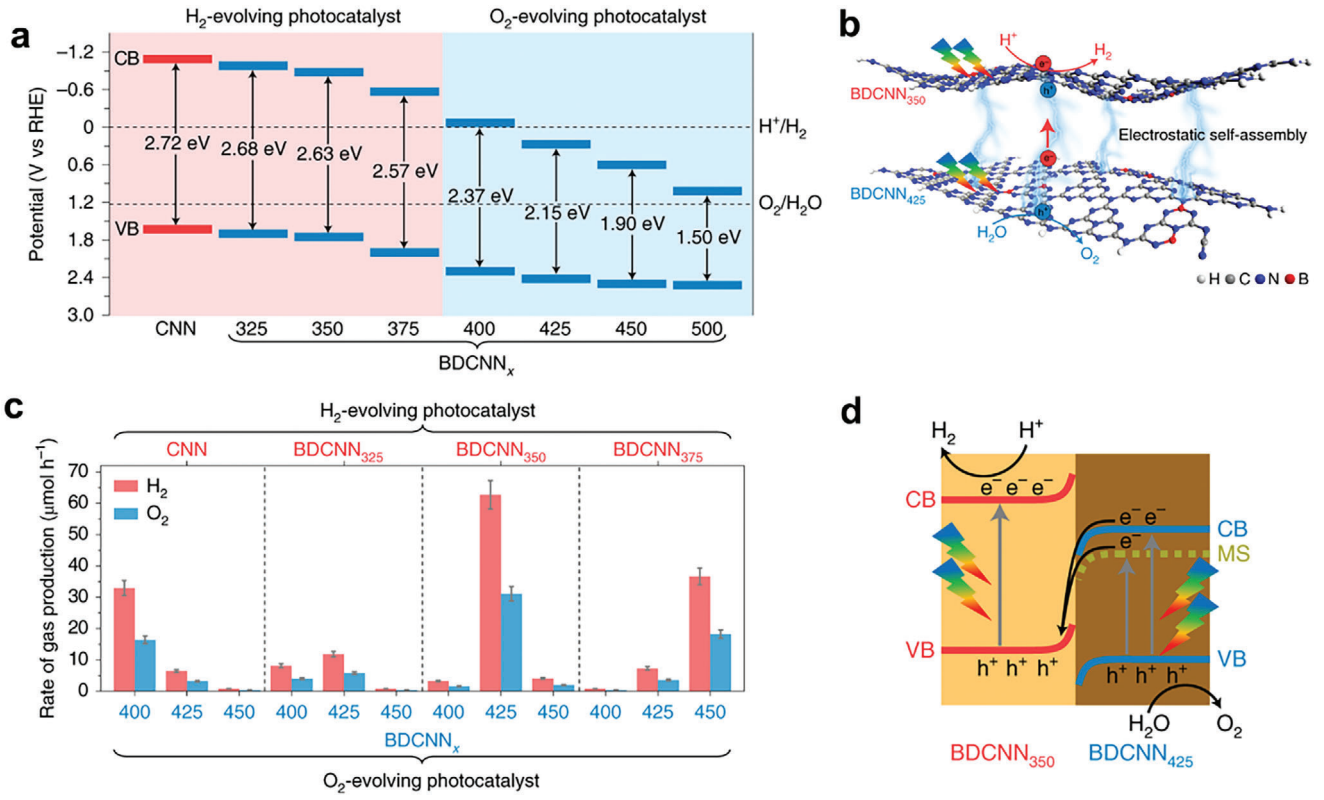

Figure 5. a) Band structure alignments for CNN and BDCNN$_x$ (x = 325, 350, 375, 400, 425, 450 and 500 °C). b) Interfacial charge property diagram. c) The overall water-splitting performance of different Z-scheme heterostructures (40 mg), self-assembled from one H_2-evolving component and one O_2-evolving component, under UV-vis light irradiation. d) Charge transfer process in BDCNN$_{350}$/BDCNN$_{425}$ upon light irradiation. Reproduced with permission.[74] Copyright 2021, Springer Nature.

6.2. Interfacial Binding

In heterojunction photocatalysts, the interface provides channels for charge transfer.[75] Large interfacial contacts and tight interfacial binding are two important parametric indicators for photocatalyst interfaces.[76] Large interfacial contacts can generate abundant charge transfer and trapping channels. A tight interfacial contact can promote the flow and migration of photogenerated carriers, while poor interfacial contact is like erecting a "wall" between two heterojunctions, which severely hinders the charge flow.[77]

Vacancies can result in coordination unsaturation, while interstitial and substitutional defects disturb the local coordination environment.[78] Furthermore, point defects can produce localized state electrons. These alterations can modulate interfacial contacts at the atomic level.[18a] Point defects act as anchoring sites for binding to other semiconductors and can create unique interfacial structures.[79] By modulating the type and number of point defects, the area, shape, and binding force of the interface can be adjusted to construct compact interfaces with large contact areas and low resistance.[70] This in turn shortens the transport distance of photogenerated carriers.

Wang et al. prepared Z-scheme photocatalysts consisting of S vacancy-rich $ZnIn_2S_4$ (S_v-$ZnIn_2S_4$) and $MoSe_2$.[80] The abundant coordinated unsaturated S atoms can act as anchoring sites for Mo atoms, promoting the formation of Mo-S bonds and the in situ growth of $MoSe_2$ on the surface of S_v-$ZnIn_2S_4$ (**Figure 6a**). The density functional theory (DFT) calculations indicate the tight chemical bonding between Mo and S, and the electron transfer from S_v-$ZnIn_2S_4$ to $MoSe_2$ at the tight heterointerface (Figure 6b,c). The Mo—S bonds generated at the interface provide a fast channel for charge transfer from $MoSe_2$ to S_v-$ZnIn_2S_4$, which further accelerates the rapid separation of photogenerated charges in this Z-scheme photocatalyst (Figure 6d). Therefore, the photocatalyst exhibits an apparent quantum yield of 76.48% and a high H_2 production rate of 63.21 mmol g^{-1} h^{-1} under 420 nm monochromatic light.

6.3. Built-in Electric Fields

Photogenerated electrons and holes need to be separated from the inside of photocatalysts and then transferred to the surface (over a distance in the range of nanometer to micrometer) to participate in the redox reaction.[81] A built-in electric field can provide the driving force to facilitate the efficient separation and transfer of photogenerated charges.[50a] For heterojunction photocatalysts, due to the difference in Fermi energies (E_f) of the semiconductors, during the equilibrium process, electron migration occurs at the heterojunction interface until E_f of the two semiconductors are the same. At this point, a built-in electric field is established and the interfacial energy band bends. The

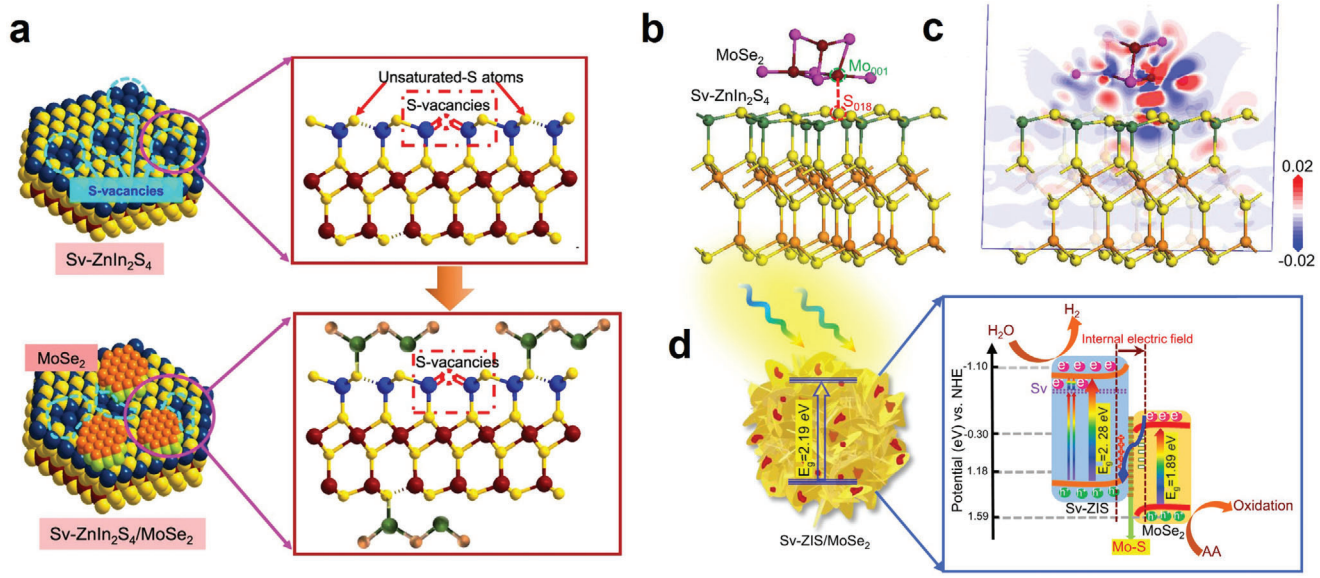

Figure 6. a) Schematic presentation of S_v-$ZnIn_2S_4/MoSe_2$ heterostructure. b) The optimized structure and c) the side view of the charge density difference of S_v-$ZnIn_2S_4/MoSe_2$ heterostructure. d) Photocatalytic reaction mechanism of S_v- $ZnIn_2S_4/MoSe_2$ under light irradiation. Reproduced with permission.[80] Copyright 2021, Springer Nature.

formation of the built-in electric field modulates the carrier migration behavior at the interface, which in turn affects the efficiency of photogenerated charge separation and transfer.[82] Differences in E_f between heterojunctions tend to influence the strength and direction of the interfacial electric field, driving charge transfer across the interfaces.[2b]

By definition, E_f refers to the highest energy level filled with electrons in the energy band of a solid at absolute zero temperature, and E_f exhibits a positive correlation with the concentration of carriers,[83] as described in Equation (2):[84]

$$E_f = E_i + kTln\frac{N_D}{n_i} \quad (2)$$

where E_i is approximated as the intrinsic E_f (located at the center of the bandgap), k is Boltzmann constant, T is temperature, N_D is the donor impurity concentration, and n_i is the intrinsic carrier concentration (a constant at a specific temperature). It can be deduced that E_f rises in the direction of CB if additional electron donors are present. Therefore, the introduction of point defects provides a way to modulate the interfacial E_f and thus manipulate the interfacial charge migration.

Based on this rationale, researchers have carried out a series of explorations, which have confirmed that the introduction of dopants can controllably regulate E_f and thus change the strength of the built-in electric field. Zhang et al. reported that by optimizing the doping concentration of V in In_2S_3 and the size of CdTe quantum dots, E_f difference between the two can be achieved continuously (**Figure 7a**).[85] The calculated electrostatic potential difference confirms that the difference of E_f between V-In_2S_3 and CdTe becomes gradually significant with the increasing V doping, thereby enhancing the built-in electric field intensity (Figure 7b). Electron transfer takes place from V-In_2S_3 to CdTe until E_f reaches equilibrium, accompanied by the formation of a space charge region (Figure 7c,d). The internal quantum efficiency is 114% at 350 nm and the STH reaches as high as 1.31% in the optimal sample (CdTe-4.2/V-In_2S_3-3) for photocatalytic H_2 production (Figure 7e).

After the formation of conventional heterojunction, the photogenerated electrons and holes tend to flow to the side with lower thermodynamic CB and VB energies, which weakens the reduction and oxidation efficiency of photogenerated electrons and holes. The construction of a Z-scheme heterojunction can effectively solve this problem. However, it is challenging to precisely control the directional migration of photogenerated charges at the interface of Z-scheme heterojunction. It has been shown that the strategy of modulating WF (The value of WF is equal to the difference between the vacuum energy level and E_f) by using vacancy defects can switch the photogenerated charge transfer path to the Z-scheme type. Sun et al. reported that the WF value of $BiVO_4$ can be altered by controlling the concentration of O vacancies.[86] When the O vacancy content in $BiVO_4$ is reduced from 8.9% to 3.8%, its WF can be altered from less than polymeric carbon nitride (PCN) to greater than PCN. As a result, the direction of interfacial energy band bending in the space charge region is reversed, and the type of the heterojunction changes from type II to Z-scheme. The common Type II $BiVO_4$/PCN cannot undergo water decomposition, whereas the solar-driven pure water decomposition is successfully realized in the Z-scheme $BiVO_4$-100/PCN photocatalyst.

6.4. Interfacial Charge Transfer Kinetics

Interfacial charge transfer kinetics is a critically important microscopic process.[87] The charge transfer kinetic behavior of heterojunction interfaces is closely related to the band structure, interface structure, doping, and other properties.[45] In recent years,

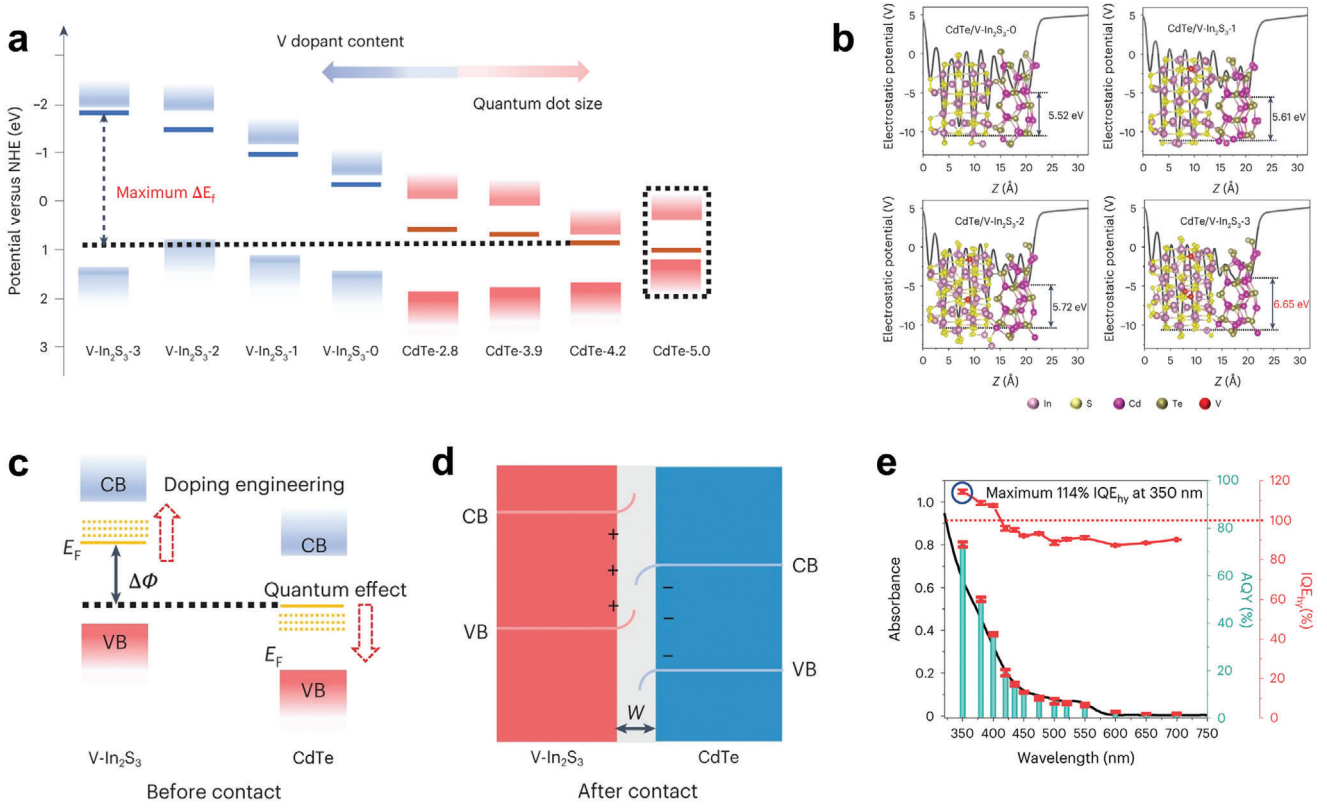

Figure 7. a) A schematic illustration of the changes in the energy band structure resulting from dopant engineering and the quantum effect. b) The calculated electrostatic potential difference for CdTe/V-In_2S_3 hybrids with different V doping (inset images: configuration of CdTe/V-In_2S_3 hybrids). *Z* is the position along the *z*-axis. c) Schematic illustration of the energy band structure of CdTe and V-In_2S_3 before contact. d) Schematic illustration of the energy band structure of CdTe and V-In_2S_3 hybrids in contact. e) The photocatalytic H_2 generation performance and absorption spectrum of CdTe-4.2/V-In_2S_3-3 hybrids. Reproduced with permission.[85] Copyright 2023, Springer Nature.

researchers have conducted studies on the charge transfer process of interfaces containing point defects, uncovering their fundamental principles. These insights provide important theoretical support for improving the electron-hole separation and photoconversion efficiency of heterojunction interfaces.

Xu et al. found that the defect states in TiO_2/Ce_2S_3 heterojunction play an important role in the charge transfer process.[88] After illumination, the photogenerated electrons that are excited to the CB of TiO_2 may subsequently enter into the impurity energy level via decay. The photogenerated electrons trapped in the impurity state will then be slowly released to recombine with the photogenerated holes left in the VB in Ce_2S_3. In this way, the lifetime of the charge carriers can be prolonged. The rapid electron trapping and timely charge separation inside TiO_2/Ce_2S_3 effectively suppress the electron-hole recombination, and it also supports the formation of an S-scheme heterojunction structure between TiO_2 and Ce_2S_3.

Wei et al. revealed the role of O vacancies in the photocatalytic oxygen evolution (OER) reaction in WO_3-Pt Schottky junction photocatalysts using ultrafast transient absorption spectroscopy (fs-TAS).[89] It was found that the electron-trapping states generated by O vacancies play an important role in charge transfer. The trap states are easier to form due to the presence of O vacancies, which trap a portion of the photogenerated electrons excited into the CB of WO_3 and inhibit the direct recombination of photogenerated carriers in WO_3. Subsequently, the photogenerated electrons trapped in the defect state are transferred to the co-catalyst Pt. Through this charge transfer way, the carrier lifetime can be extended and the activity of photocatalytic OER reaction is enhanced.

Li et al. successfully realized the modulation of the charge transfer path by using point defects.[58] By introducing abundant $W^{5/4+}$ low-valent metal defect sites at the $WO_{3-x}/GdCrO_3$ interface, the type of this heterojunction can be successfully transformed from type III to bridged type III (bridged by an interfacial defect band). Point defect sites introduced in the interface can serve as a bridge for thermally induced charge storage, secondary excitation, and interband transfer, thus realizing the effective separation of photogenerated charges under photothermal conditions. The heterojunction demonstrates excellent performance in photothermal catalyzed volatile organic compounds purification and CO_2 reduction.

6.5. Redox Reactions on Surfaces

In heterojunction photocatalysts, chemical interactions between interfacial atoms can modulate the charge density around the active sites and regulate the redox reactions on the surface.[90] Point defects in heterojunctions help tailor interface characteristics at

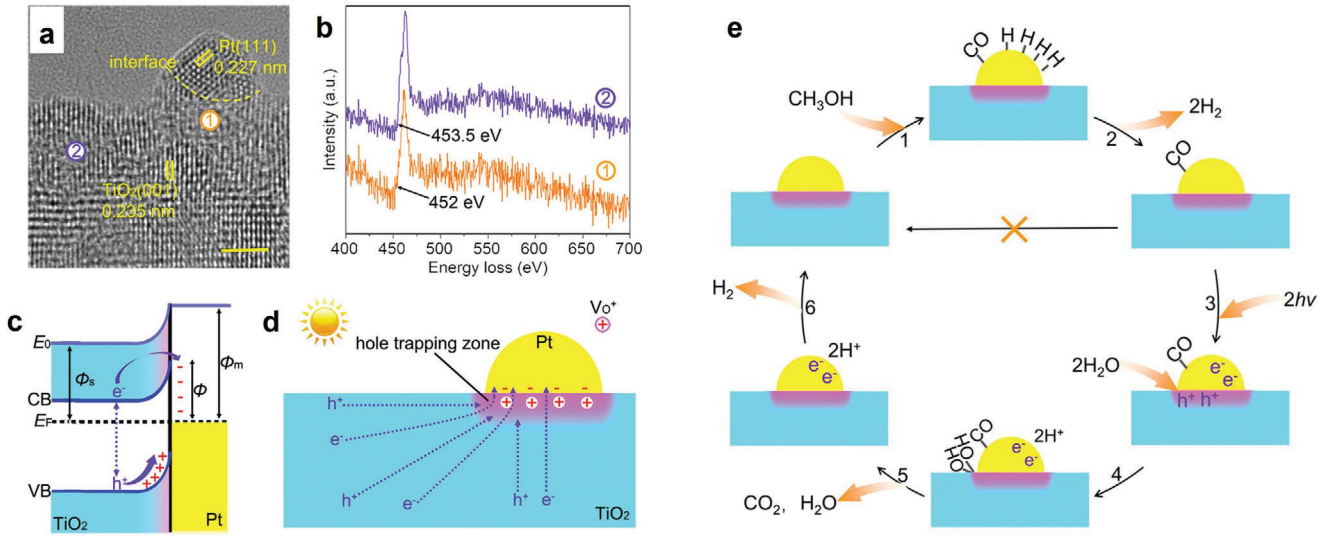

Figure 8. a) HRTEM image of 5 wt.% Pt/TiO_2 catalyst. b) Ti L-edge EELS of TiO_2 substrate near the interface (1, yellow line) and far away from the interface (2, blue line) in the HRTEM image. c) Energy diagram of the Pt/TiO_2 with O vacancies concentrated at the interface. d) Scheme for trapping of photogenerated charges after concentrating O vacancies only at the Pt-TiO_2 interface. e) Unique interface-triggered photocatalytic cycle. Reproduced with permission.[91] Copyright 2019, National Academy of Sciences.

the atomic level and can also participate in the reaction as active sites. Additionally, heterostructures containing point defects can address the issue of the metastability of defect structures.[18a] The combination of point defects and heterojunctions can enhance the transport of surface photogenerated carriers, promote the effective separation of photogenerated carriers, enhance the number of surface active sites, and regulate the surface reaction kinetics, thus realizing efficient photocatalytic surface redox reactions.

Point defect engineering can modulate the photocatalytic surface reaction pathways. For example, Zhou et al. obtained a high concentration of O vacancies at the Pt-TiO_2 interface by a simple photo-deposition method (**Figure** 8a,b).[91] High concentrations of O vacancies at the Pt-TiO_2 interface can lower the Schottky barrier height to improve the electron injection (Figure 8c). As a result, electrons are easier to be trapped by the Pt, while holes are attracted toward the perimeter of the Pt nanoparticles at the same time (Figure 8d). The presence of O vacancies facilitates the CO oxidation reaction of photogenerated holes at the Pt-TiO_2 interface, alleviating the blockage of adsorbed CO to the active sites on Pt, which leads to the continuous decomposition of alcohols on Pt into CO_{ads} and H_2 (Figure 8e). O vacancies trigger unusual reaction paths, allowing alcohols to no longer act as sacrificial reagents but rather as promising substances for H_2 storage.

Point defect doping can directly introduce active sites. Chao et al. ingeniously designed a series of In_2O_3-$ZnIn_2Se_4$ Z-scheme nanosheet photocatalysts, which greatly enhanced the rate of photocatalytic H_2 production.[92] By adding Mo atoms (in the form of Mo—Se bond) to the Z-scheme In_2O_3-$ZnIn_2Se_4$ photocatalysts, In_2O_3-$ZnIn_2Se_4$-Mo was obtained which could achieve further optimization of the photocatalytic performance. Under visible light, the H_2 production rate of In_2O_3-$ZnIn_2Se_4$-Mo can be as high as 6.95 mmol g^{-1} h^{-1}, which is 21.7 and 232.6 times higher than that of the In_2O_3-$ZnIn_2Se_4$ nanosheets and In_2O_3 nanosheets, respectively. This study combined elemental doping with controllable surface engineering to achieve synergistic modulation of active sites and surface adsorption properties, which led to the realization of efficient photocatalytic H_2 production performance.

6.6. Point Defects Induced Unique Physical Properties

6.6.1. Defects Induced Localized Surface Plasmon Resonance (LSPR)

LSPR is an optical property in nanoparticles, which refers to the collective oscillation of free carriers driven by incident light. At a certain frequency, the oscillations of free carriers resonate with the incident light.[93] Plasmonic photocatalysts with large absorption cross sections and strong localized field enhancement, as well as the ability to generate hot electrons and hot holes, show attractive prospects for improving photocatalytic efficiency.[94] Conventional metal plasma materials such as Au, Ag, and other noble metals have inherent limitations that lead to the underutilization of hot electrons and difficulties with the recombination of hot charge carriers.[95] With further studies, researchers have found that doped semiconductor nanoparticles with suitable concentrations of free carriers also have the LSPR effect, such as $Cu_{2-x}S$,[96] MoO_{3-x},[97] and WO_{3-x}[98] semiconductors with high densities of free charge carriers. Semiconductor plasmonic materials have tunable properties, and their carrier densities can be easily tuned by changing the doping concentration for enhanced utilization of hot electrons and improved photocatalytic performance.[99]

Lu et al. compounded $ZnIn_2S_4$ nanosheets on hierarchical $W_{18}O_{49}$ micro flowers (WO/ZIS), which possessed excellent H_2 production performance, with the H_2 yield reaching 902.57 µmol in 3 h under simulated sunlight.[100] The Z-scheme heterojunction was constructed and the separation of electron-hole pairs was accelerated. More importantly, O-deficient $W_{18}O_{49}$ with LSPR effect plays an important role in enhancing the

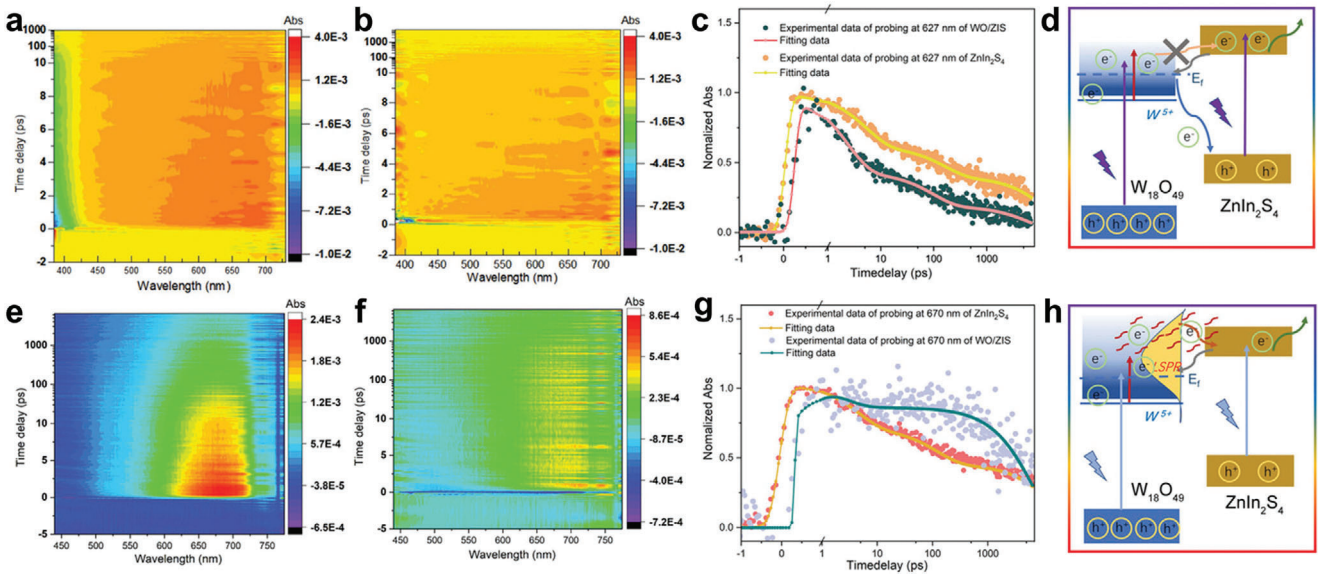

Figure 9. Pseudocolor fs-TAS plots of (a) $ZnIn_2S_4$ and (b) WO/ZIS under 360 nm irradiation. c) TA dynamics of $ZnIn_2S_4$ and WO/ZIS under 360 nm irradiation fitted by two-exponential and three-exponential functions. d) Schematic diagram of electron transition of WO/ZIS under 360 nm irradiation. Pseudocolor fs-TAS plots of e) $ZnIn_2S_4$ and f) WO/ZIS under 400 nm irradiation. g) fs-TAS dynamics of pure $ZnIn_2S_4$ and WO/ZIS under 400 nm irradiation fitted by two-exponential and three-exponential functions. h) Schematic diagram of electron transition of WO/ZIS under 400 nm irradiation. Reproduced with permission.[100] Copyright 2022, John Wiley & Sons.

performance of the photocatalyst. fs-TAS was conducted under 360 nm irradiation (**Figure 9**a–c), confirming that the composite exhibits a Z-scheme charge transfer mechanism (Figure 9d). Charge transfer kinetics of WO/ZIS show a difference under 400 nm irradiation according to fs-TAS (Figure 9e–g). In this excitation process, $W_{18}O_{49}$ undergoes the LSPR effect, during which high-energy hot electrons are transferred to the CB of $ZnIn_2S_4$. This process induced by LSPR extends the light absorption range and increases the concentration of photogenerated carriers (Figure 9h).

6.6.2. Photothermal Effect

Thermocatalysis is a process in which the entire reaction system is heated, and the reaction is initiated when the system temperature reaches the thermodynamic activation energy for the reaction.[101] By integrating the reaction characteristics of photocatalysis and thermocatalysis, and utilizing the absorption of the full solar spectrum, the coupling of thermochemical and photochemical processes can be triggered to surpass the activity of a single photocatalysis or thermocatalysis alone, which is an effective strategy for upgrading photocatalysis.[102] The conversion of solar energy into photothermochemical reactions has also become a research focus for a new generation of solar photocatalysis.

Converting light into heat is one of the main methods to achieve efficient photothermal catalysis.[103] Generally, metals,[104] semiconductors,[105] and carbon materials[106] are used as photothermal conversion materials due to their ability to convert light energy partially or completely into heat energy, which is widely used in the fields of photothermal CO_2 reduction, H_2 production, and photothermal cancer therapy.

Due to the limitation of the intrinsic band structure, pure semiconductor photocatalysts have low absorption in the near-infrared (NIR) region, and it has been demonstrated that point defects can enhance the light absorption property of semiconductors and improve their photothermal performance.[107] For example, hydrogenated black TiO_2 and S-doped TiO_2 have excellent absorption in the NIR region and have shown excellent application outcomes in photothermal cancer therapy.[108]

Tang et al. designed 1T-WS_2 (with S vacancies) as a photothermal catalyst, which was composited with CdS to form a heterojunction, demonstrating an outstanding H_2 production rate.[109] It was found that S vacancy was both an adsorption site for *H and a trapping site for photogenerated electrons, which could rapidly reduce the adsorbed *H to H_2. More importantly, the introduction of S vacancy in 1T-WS_2 not only enlarged the photo-response range, but also promoted the reaction kinetics, and accelerated the directional migration of electrons from CdS to S vacancy by inducing a photothermal effect.

7. Challenges and Perspectives

The combination of point defects and heterojunction engineering has demonstrated the potential to realize efficient solar energy utilization. Point defect structures, such as vacancies and doping, have important effects on the properties of heterojunction photocatalysts, including energy band modulation, interfacial bonding, and charge transfer processes. This paper summarizes the contribution of point defects to the photocatalytic performance of heterojunction photocatalysts and the underlying mechanisms. Although many types of point defect heterojunction photocatalysts have been

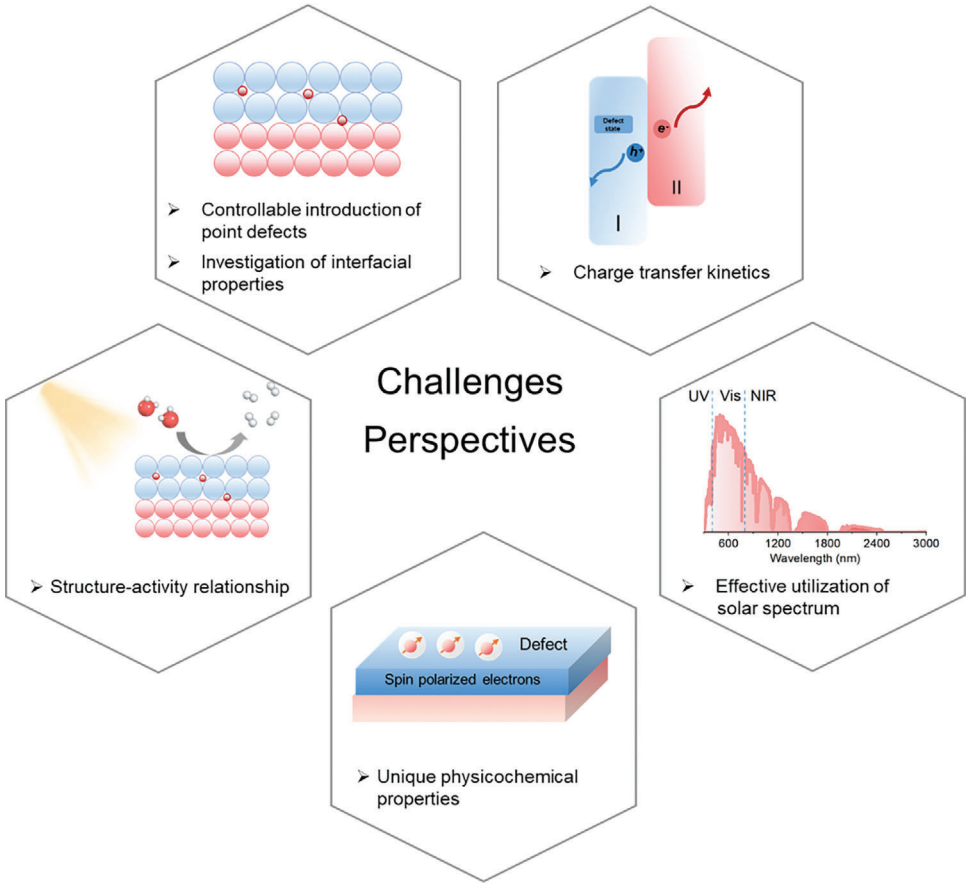

Figure 10. Future development paths for highly efficient point defects incorporated heterojunction photocatalysts.

developed, their efficiencies are still insufficient for practical applications. The fundamental study and rational utilization of point defects is still in its infancy. Therefore, to further advance this field, some future perspectives are proposed below (**Figure 10**).

7.1. Controllable Introduction of Point Defects and Investigations of Interfacial Properties

Achieving precise regulation of point defects is the cornerstone of their effective utilization in heterojunction photocatalysts. Therefore, it is essential to compensate for the limitations of existing synthesis methods and develop multiple methods to realize the precise control of the type, concentration, and distribution of point defects.

After achieving controlled manipulation of point defects, it is necessary to combine multiple characterization methods with improved detection resolution and accuracy to semi-quantitatively or even quantitatively verify how different types and numbers of defects exist and function at the interface. Moreover, the influence of different forms of point defects on the interfacial characteristics, band structure, built-in electric field, etc. should be investigated. Ultimately, more efforts should be made to harness point defects for the strategic synthesis of heterojunction photocatalysts to controllably adjust the geometric configuration and electronic properties of the interface, providing a strong driving force for charge transfer.

7.2. Probing the Structure-Activity Relationship of Point Defect Heterojunctions

The complexity of the heterojunction structure and the photocatalytic reaction process makes it quite challenging to deeply cognize the mechanism of point defects in the reaction. Consequently, it is imperative to employ advanced characterization techniques. For instance, in situ observations with high spatial and temporal resolutions can be employed to elucidate the structural evolution of point defects and the dynamics of the photocatalytic reaction. This will foster a deeper comprehension of the structure-activity relationship between point defects in heterojunctions and photocatalytic reactions and thereby guide the design of point defect heterojunctions for specific photocatalytic reactions.

Additionally, for different photocatalytic reactions, specific doped elements can provide reactive sites.[90,110] Therefore, point defect engineering can be utilized to create catalytic active centers at the atomic scale. By leveraging the coupled effects of point defects as active centers and their regulatory influence on factors such as band structure, charge separation, and transfer, a

synergistic optimization of photocatalytic reactions in terms of both thermodynamics and kinetics may be achieved.

7.3. Effective Utilization of Solar Spectrum by Point Defect Broadened Heterojunction Photocatalysts

The energy of NIR light constitutes nearly half of the total solar energy, and the effective capturing of this portion of light is essential for the efficient utilization of solar energy. The presence of point defects significantly broadens the solar energy absorption range, yet, due to the lower energy photons in the NIR region, they are incapable of directly engaging in redox reactions. Heterojunction photocatalysts containing point defects are undoubtedly a potential candidate for harvesting NIR light. Point defects serve to extend the absorption range of the solar spectrum, while the special photogenerated charge transfer pathway within the S-scheme heterojunction can endow the photogenerated carriers with sufficient redox ability, which can be regarded as a way to kill two birds with one stone. Based on this, efficient and novel NIR-responsive heterojunction photocatalysts should be investigated. A potential strategy involves the introduction of point defects to form a narrow bandgap semiconductor, which can be coupled with a visible light-responsive semiconductor to create a visible/NIR-responsive heterojunction. In addition, point defects can also induce the LSPR effect in photocatalysts, which can exceptionally absorb and convert NIR light. Consequently, integrating photocatalysts with the LSPR effect with visible-responsive photocatalysts can also be a feasible strategy for harvesting NIR light.

7.4. Mechanisms of Point Defects on Charge Transfer Kinetics

The rapid recombination of photogenerated charges has always been a key factor constraining the activity of photocatalytic reactions. However, limited by the rapidity and complexity of the process, its interpretation remains vague and inadequate. In particular, the dynamics of photogenerated carrier separation and transport within the heterojunction, when point defects are present, have yet to be thoroughly elucidated. If this process can be profoundly interpreted, point defects can be utilized to precisely steer the pathways of charge transfer. For example, modulating Type II to S-scheme heterojunctions to obtain photogenerated carriers with higher redox capabilities.

So far, fs-TAS,[111] in situ light-illuminated X-ray photoelectron spectroscopy[112] and in situ scanning probe microscopy[113] have successfully detected the photogenerated charge transfer mechanism of photocatalysts. However, there is still a lack of in-depth understanding of the transient process and full-time evolution of the photogenerated charges at the heterojunction interface, especially the role of point defects in the charge transfer process. In the future, the focus will be on improving the spatial resolution and sensitivity of the above detection techniques and combining them with theoretical simulations to further enhance the understanding of the effect of point defects on the dynamics of photogenerated charge transfer. This will bridge the gap between the structure of the point defect heterojunctions and their photocatalytic activity.

7.5. Unique Physicochemical Properties Induced by Point Defects

Point defects induce a series of unique physicochemical properties in semiconductors, such as the LSPR effect, which has been extensively studied in single photocatalysts. Exploring the creation and relaxation mechanism of hot electrons induced by point defects in heterojunctions and improving the utilization efficiency of hot electrons will be more helpful for defects to participate in photocatalytic reactions. Except this, it has been demonstrated that different electronic spin polarization structures can influence photocatalytic reactions.[114] The formation of metal vacancies can regulate spin polarization in semiconductors,[115] enhancing the efficiency of photo-induced charge separation and surface reactions.

The special physicochemical phenomena generated by point defect engineering can motivate the introduction of its advantages into heterojunction photocatalysts. This is aimed at enhancing charge utilization and inducing novel reaction mechanisms, with the expectation of achieving excellent photocatalytic activity.

8. Conclusion

Overall, point defects have demonstrated distinctive benefits for enhancing the performance of heterojunction photocatalysts, with the light absorption capability, charge separation efficiency, and surface reaction activity of photocatalysts being well regulated. Additionally, notable advancements have been achieved in the application and understanding of point defects. Nevertheless, the development of efficient and stable heterojunction photocatalysts that incorporate point defects still faces many obstacles which include precise controlling of the type and concentration of point defects, unexplored regulatory patterns of point defects on the interfacial properties of heterojunction photocatalysts, and unexplored mechanisms of point defects in affecting the charge separation and transport in heterojunction photocatalysts. This review expects to elucidate the potential impact of incorporating point defects in heterojunction photocatalysts, emphasizing their crucial role in enhancing the performance of photocatalysts and outlining future research directions in this field.

Acknowledgements

This project was financially supported by The Hong Kong Polytechnic University (1-CD6V, 1-CD8V and Q-CDBG).

Conflict of Interest

The authors declare no conflict of interest.

Keywords

charge transfer, heterointerface, photocatalysis, point defects, heterojunctions

Received: May 13, 2024
Revised: June 25, 2024
Published online: July 22, 2024

[1] a) P. Zhou, I. A. Navid, Y. Ma, Y. Xiao, P. Wang, Z. Ye, B. Zhou, K. Sun, Z. Mi, *Nature* **2023**, *613*, 66; b) A. Fujishima, K. Honda, *Nature* **1972**, *238*, 37; c) S. Linic, P. Christopher, D. B. Ingram, *Nat. Mater.* **2011**, *10*, 911.
[2] a) T. Liu, Z. Pan, J. J. M. Vequizo, K. Kato, B. Wu, A. Yamakata, K. Katayama, B. Chen, C. Chu, K. Domen, *Nat. Commun.* **2022**, *13*, 1034; b) L. Zhang, J. Zhang, H. Yu, J. Yu, *Adv. Mater.* **2022**, *34*, 2107668.
[3] F. He, W. Jeon, W. Choi, *Nat. Commun.* **2021**, *12*, 2528.
[4] H. Hou, X. Zeng, X. Zhang, *Angew. Chem., Int. Ed.* **2020**, *59*, 17356.
[5] J. Kosco, M. Bidwell, H. Cha, T. Martin, C. T. Howells, M. Sachs, D. H. Anjum, S. Gonzalez Lopez, L. Zou, A. Wadsworth, W. Zhang, L. Zhang, J. Tellam, R. Sougrat, F. Laquai, D. M. DeLongchamp, J. R. Durrant, I. McCulloch, *Nat. Mater.* **2020**, *19*, 559.
[6] M. Bonchio, J. Bonin, O. Ishitani, T.-B. Lu, T. Morikawa, A. J. Morris, E. Reisner, D. Sarkar, F. M. Toma, M. Robert, *Nat. Catal.* **2023**, *6*, 657.
[7] I. Ghosh, J. Khamrai, A. Savateev, N. Shlapakov, M. Antonietti, B. König, *Science* **2019**, *365*, 360.
[8] S. Fang, X. Lyu, T. Tong, A. I. Lim, T. Li, J. Bao, Y. H. Hu, *Nat. Commun.* **2023**, *14*, 1203.
[9] X. Xin, Y. Zhang, R. Wang, Y. Wang, P. Guo, X. Li, *Nat. Commun.* **2023**, *14*, 1759.
[10] Q. Wu, J. Cao, X. Wang, Y. Liu, Y. Zhao, H. Wang, Y. Liu, H. Huang, F. Liao, M. Shao, Z. Kang, *Nat. Commun.* **2021**, *12*, 483.
[11] J. Qi, W. Zhang, R. Cao, *Adv. Energy Mater.* **2017**, *8*, 1701620.
[12] J. Di, C. Chen, Y. Wu, H. Chen, J. Xiong, R. Long, S. Li, L. Song, W. Jiang, Z. Liu, *Adv. Mater.* **2024**, *36*, 2401914.
[13] Z. Chen, J. Wang, M. Hao, Y. Xie, X. Liu, H. Yang, G. I. N. Waterhouse, X. Wang, S. Ma, *Nat. Commun.* **2023**, *14*, 1106.
[14] B. Zhu, J. Sun, Y. Zhao, L. Zhang, J. Yu, *Adv. Mater.* **2024**, *36*, 2310600.
[15] S. Wang, M. Xu, T. Peng, C. Zhang, T. Li, I. Hussain, J. Wang, B. Tan, *Nat. Commun.* **2019**, *10*, 676.
[16] a) G. L. Qian, Q. Xie, Q. Liang, X. Y. Luo, Y. X. Wang, *Phys. Rev. B.* **2023**, *107*, 155306; b) Y. Wang, X. H. Liu, Q. Wang, M. Quick, S. A. Kovalenko, Q. Y. Chen, N. Koch, N. Pinna, *Angew. Chem., Int. Ed.* **2020**, *59*, 7748.
[17] a) F. F. Abdi, L. Han, A. H. Smets, M. Zeman, B. Dam, R. van de Krol, *Nat. Commun.* **2013**, *4*, 2195; b) J. Fu, Z. Fan, M. Nakabayashi, H. Ju, N. Pastukhova, Y. Xiao, C. Feng, N. Shibata, K. Domen, Y. Li, *Nat. Commun.* **2022**, *13*, 729; c) S. Li, W. Xu, L. Meng, W. Tian, L. Li, *Small Sci.* **2022**, *2*, 2100112.
[18] a) S. Zhang, Y. Si, B. Li, L. Yang, W. Dai, S. Luo, *Small* **2021**, *17*, 2004980; b) Y. Sun, H. Ji, Y. Sun, G. Zhang, H. Zhou, S. Cao, S. Liu, L. Zhang, W. Li, X. Zhu, H. Pang, *Angew. Chem., Int. Ed.* **2024**, *63*, 202316973.
[19] Y. Liu, X. Zheng, Y. Fang, Y. Zhou, Z. Ni, X. Xiao, S. Chen, J. Huang, *Nat. Commun.* **2021**, *12*, 1686.
[20] a) A. Gottscholl, M. Kianinia, V. Soltamov, S. Orlinskii, G. Mamin, C. Bradac, C. Kasper, K. Krambrock, A. Sperlich, M. Toth, I. Aharonovich, V. Dyakonov, *Nat. Mater.* **2020**, *19*, 540; b) Y. Zheng, T. J. Slade, L. Hu, X. Y. Tan, Y. Luo, Z.-Z. Luo, J. Xu, Q. Yan, M. G. Kanatzidis, *Chem. Soc. Rev.* **2021**, *50*, 9022.
[21] C. Bie, H. Yu, B. Cheng, W. Ho, J. Fan, J. Yu, *Adv. Mater.* **2021**, *33*, 2003521.
[22] C. Feng, L. Tang, Y. Deng, J. Wang, J. Luo, Y. Liu, X. Ouyang, H. Yang, J. Yu, J. Wang, *Adv. Funct. Mater.* **2020**, *30*, 2001922.
[23] R. Chen, Z. Ren, Y. Liang, G. Zhang, T. Dittrich, R. Liu, Y. Liu, Y. Zhao, S. Pang, H. An, C. Ni, P. Zhou, K. Han, F. Fan, C. Li, *Nature* **2022**, *610*, 296.
[24] H. Shen, M. Yang, L. Hao, J. Wang, J. Strunk, Z. Sun, *Nano Res.* **2021**, *15*, 2773.
[25] a) J. Zhang, J. Willis, Z. Yang, Z. Sheng, L.-S. Wang, T.-L. Lee, L. Chen, D. O. Scanlon, K. H. L. Zhang, *Phys. Rev. B.* **2022**, *106*, 205305; b) Y. Xu, C. Horn, J. Zhu, Y. Tang, L. Ma, L. Li, S. Liu, K. Watanabe, T. Taniguchi, J. C. Hone, J. Shan, K. F. Mak, *Nat. Mater.* **2021**, *20*, 645.
[26] R. Li, T. Takata, B. Zhang, C. Feng, Q. Wu, C. Cui, Z. Zhang, K. Domen, Y. Li, *Angew. Chem., Int. Ed.* **2023**, *62*, 202313537.
[27] S. Fang, M. Rahaman, J. Bharti, E. Reisner, M. Robert, G. A. Ozin, Y. H. Hu, *Nat. Rev. Methods Primers* **2023**, *3*, 61.
[28] D. Thomas, Y. Asiri, N. Drummond, *Phys. Rev. B.* **2022**, *105*, 184114.
[29] B. Zhao, Y. Du, Z. Yan, L. Rao, G. Chen, M. Yuan, L. Yang, J. Zhang, R. Che, *Adv. Funct. Mater.* **2022**, *33*, 2209924.
[30] R. Yang, D. Yang, M. Wang, F. Zhang, X. Ji, M. Zhang, M. Jia, X. Chen, D. Wu, X. J. Li, Y. Zhang, Z. Shi, C. Shan, *Adv. Sci.* **2023**, *10*, 2207331.
[31] L. C. Yin, W. D. Liu, M. Li, D. Z. Wang, H. Wu, Y. Wang, L. Zhang, X. L. Shi, Q. Liu, Z. G. Chen, *Adv. Funct. Mater.* **2023**, *33*, 2301750.
[32] a) R. E. Blackwell, F. Zhao, E. Brooks, J. Zhu, I. Piskun, S. Wang, A. Delgado, Y. L. Lee, S. G. Louie, F. R. Fischer, *Nature* **2021**, *600*, 647; b) H. L. Stern, Q. Gu, J. Jarman, S. E. Barker, N. Mendelson, D. Chugh, S. Schott, H. H. Tan, H. Sirringhaus, I. Aharonovich, M. Atature, *Nat. Commun.* **2022**, *13*, 618.
[33] T. Xing, C. Zhu, Q. Song, H. Huang, J. Xiao, D. Ren, M. Shi, P. Qiu, X. Shi, F. Xu, L. Chen, *Adv. Mater.* **2021**, *33*, 2008773.
[34] N. C. Frey, D. Akinwande, D. Jariwala, V. B. Shenoy, *ACS Nano* **2020**, *14*, 13406.
[35] W. Gao, S. Li, H. He, X. Li, Z. Cheng, Y. Yang, J. Wang, Q. Shen, X. Wang, Y. Xiong, Y. Zhou, Z. Zou, *Nat. Commun.* **2021**, *12*, 4747.
[36] S. C. Erwin, L. Zu, M. I. Haftel, A. L. Efros, T. A. Kennedy, D. J. Norris, *Nature* **2005**, *436*, 91.
[37] W. Lei, Y. Yu, H. Zhang, Q. Jia, S. Zhang, *Mater. Today* **2022**, *52*, 133.
[38] C. Han, B. K. Kundu, Y. Liang, Y. Sun, *Adv. Mater.* **2024**, *36*, 2307759.
[39] Y. Zhang, C. Pan, G. Bian, J. Xu, Y. Dong, Y. Zhang, Y. Lou, W. Liu, Y. Zhu, *Nat. Energy* **2023**, *8*, 361.
[40] A. Kozhakhmetov, B. Schuler, A. M. Z. Tan, K. A. Cochrane, J. R. Nasr, H. El-Sherif, A. Bansal, A. Vera, V. Bojan, J. M. Redwing, N. Bassim, S. Das, R. G. Hennig, A. Weber-Bargioni, J. A. Robinson, *Adv. Mater.* **2020**, *32*, 2005159.
[41] A. Zunger, O. I. Malyi, *Chem. Rev.* **2021**, *121*, 3031.
[42] L. Gao, C. Tang, J. Liu, L. He, H. Wang, Z. Ke, W. Li, C. Jiang, D. He, L. Cheng, X. Xiao, *Energy Environ. Mater.* **2020**, *4*, 392.
[43] J. S. Park, S. Kim, Z. Xie, A. Walsh, *Nat. Rev. Mater.* **2018**, *3*, 194.
[44] S. Kundu, A. Patra, *Chem. Rev* **2017**, *117*, 712.
[45] W. Chu, W. A. Saidi, Q. Zheng, Y. Xie, Z. Lan, O. V. Prezhdo, H. Petek, J. Zhao, *J. Am. Chem. Soc.* **2016**, *138*, 13740.
[46] C. Fu, F. Li, J. Zhang, D. Li, K. Qian, Y. Liu, J. Tang, F. Fan, Q. Zhang, X. Q. Gong, W. Huang, *Angew. Chem., Int. Ed.* **2021**, *60*, 6160.
[47] X. Jiao, Z. Chen, X. Li, Y. Sun, S. Gao, W. Yan, C. Wang, Q. Zhang, Y. Lin, Y. Luo, Y. Xie, *J. Am. Chem. Soc.* **2017**, *139*, 7586.
[48] D. Maarisetty, S. S. Baral, *J. Mater. Chem. A.* **2020**, *8*, 18560.
[49] J. Zhou, J. Zhao, R. Liu, *Appl. Catal. B. Environ.* **2020**, *278*, 119265.
[50] a) Y. Wang, J. Hu, T. Ge, F. Chen, Y. Lu, R. Chen, H. Zhang, B. Ye, S. Wang, Y. Zhang, T. Ma, H. Huang, *Adv. Mater.* **2023**, *35*, 2302538; b) R. Chen, S. Pang, H. An, T. Dittrich, F. Fan, C. Li, *Nano Lett.* **2019**, *19*, 426.
[51] Q. Guo, C. Zhou, Z. Ma, X. Yang, *Adv. Mater.* **2019**, *31*, 1901997.
[52] W. Jiang, J. Low, K. Mao, D. Duan, S. Chen, W. Liu, C. W. Pao, J. Ma, S. Sang, C. Shu, X. Zhan, Z. Qi, H. Zhang, Z. Liu, X. Wu, R. Long, L. Song, Y. Xiong, *J. Am. Chem. Soc.* **2021**, *143*, 269.
[53] X. Yu, S. F. Ng, L. K. Putri, L. L. Tan, A. R. Mohamed, W. J. Ong, *Small* **2021**, *17*, 2006851.
[54] E. Hua, S. Jin, X. Wang, S. Ni, G. Liu, X. Xu, *Appl. Catal. B. Environ.* **2019**, *245*, 733.
[55] X. Meng, S. Wang, C. Zhang, C. Dong, R. Li, B. Li, Q. Wang, Y. Ding, *ACS Catal.* **2022**, *12*, 10115.

[56] Y. Zhu, T. Wan, X. Wen, D. Chu, Y. Jiang, *Appl. Catal. B. Environ.* **2019**, *244*, 814.
[57] X. Zhao, S. Chen, H. Yin, S. Jiang, K. Zhao, J. Kang, P. F. Liu, L. Jiang, Z. Zhu, D. Cui, P. Liu, X. Han, H. G. Yang, H. Zhao, *Matter* **2020**, *3*, 935.
[58] J. Li, J. Feng, X. Guo, H. Fang, J. Chen, C. Ma, R. Li, Y. Wang, Z. Rui, *Appl. Catal. B. Environ.* **2022**, *309*, 121248.
[59] Y. Wang, X. Shang, J. Shen, Z. Zhang, D. Wang, J. Lin, J. C. S. Wu, X. Fu, X. Wang, C. Li, *Nat. Commun.* **2020**, *11*, 3043.
[60] a) Q. Wang, T. Hisatomi, Y. Suzuki, Z. Pan, J. Seo, M. Katayama, T. Minegishi, H. Nishiyama, T. Takata, K. Seki, A. Kudo, T. Yamada, K. Domen, *J. Am. Chem. Soc.* **2017**, *139*, 1675; b) Q. Wang, Y. Li, T. Hisatomi, M. Nakabayashi, N. Shibata, J. Kubota, K. Domen, *J. Catal.* **2015**, *328*, 308.
[61] a) Q. Wang, J. Warnan, S. Rodríguez-Jiménez, J. J. Leung, S. Kalathil, V. Andrei, K. Domen, E. Reisner, *Nat. Energy* **2020**, *5*, 703; b) Q. Wang, T. Hisatomi, Q. Jia, H. Tokudome, M. Zhong, C. Wang, Z. Pan, T. Takata, M. Nakabayashi, N. Shibata, Y. Li, I. D. Sharp, A. Kudo, T. Yamada, K. Domen, *Nat. Mater.* **2016**, *15*, 611.
[62] Y. Jiang, J.-F. Liao, H.-Y. Chen, H.-H. Zhang, J.-Y. Li, X.-D. Wang, D.-B. Kuang, *Chem* **2020**, *6*, 766.
[63] P. Zhou, J. Yu, M. Jaroniec, *Adv. Mater.* **2014**, *26*, 4920.
[64] P. Xia, S. Cao, B. Zhu, M. Liu, M. Shi, J. Yu, Y. Zhang, *Angew. Chem., Int. Ed.* **2020**, *59*, 5218.
[65] W. Zhang, A. R. Mohamed, W. J. Ong, *Angew. Chem., Int. Ed.* **2020**, *59*, 22894.
[66] F. Xing, C. Cheng, J. Zhang, Q. Liu, C. Chen, C. Huang, *Appl. Catal. B. Environ.* **2021**, *285*, 119818.
[67] X. Wang, C. Zhang, J. Du, X. Dong, S. Jian, L. Yan, Z. Gu, Y. Zhao, *ACS Nano* **2019**, *13*, 5947.
[68] X. Wu, Y. Zhang, K. Wang, S. Zhang, X. Qu, L. Shi, F. Du, *J. Hazard. Mater.* **2020**, *393*, 122408.
[69] M. Xu, X. Ruan, D. Meng, G. Fang, D. Jiao, S. Zhao, Z. Liu, Z. Jiang, K. Ba, T. Xie, *Adv. Funct. Mater.* **2024**, 2402330, https://doi.org/10.1002/adfm.202402330.
[70] M. Lin, H. Chen, Z. Zhang, X. Wang, *Phys. Chem. Chem. Phys.* **2023**, *25*, 4388.
[71] L. Chen, J. T. Ren, Z. Y. Yuan, *Adv. Energy Mater.* **2023**, *13*, 2203720.
[72] Q. Su, Y. Li, R. Hu, F. Song, S. Liu, C. Guo, S. Zhu, W. Liu, J. Pan, *Adv. Sustain. Syst.* **2020**, *4*, 2000130.
[73] D. Zhao, C. L. Dong, B. Wang, C. Chen, Y. C. Huang, Z. Diao, S. Li, L. Guo, S. Shen, *Adv. Mater.* **2019**, *31*, 1903545.
[74] D. Zhao, Y. Wang, C.-L. Dong, Y.-C. Huang, J. Chen, F. Xue, S. Shen, L. Guo, *Nat. Energy* **2021**, *6*, 388.
[75] S. Bai, J. Jiang, Q. Zhang, Y. Xiong, *Chem. Soc. Rev.* **2015**, *44*, 2893.
[76] H. Yu, M. Dai, J. Zhang, W. Chen, Q. Jin, S. Wang, Z. He, *Small* **2023**, *19*, 2205767.
[77] B. X. Zhou, S. S. Ding, K. X. Yang, J. Zhang, G. F. Huang, A. Pan, W. Hu, K. Li, W. Q. Huang, *Adv. Funct. Mater.* **2020**, *31*, 2009230.
[78] N. Li, Y. Zhu, F. Jiao, X. Pan, Q. Jiang, J. Cai, Y. Li, W. Tong, C. Xu, S. Qu, B. Bai, D. Miao, Z. Liu, X. Bao, *Nat. Commun.* **2022**, *13*, 2742.
[79] Y. Zhao, W. J. Jiang, J. Zhang, E. C. Lovell, R. Amal, Z. Han, X. Lu, *Adv. Mater.* **2021**, *33*, 2102801.
[80] X. Wang, X. Wang, J. Huang, S. Li, A. Meng, Z. Li, *Nat. Commun.* **2021**, *12*, 4112.
[81] Y. Hu, Y. Pan, Z. Wang, T. Lin, Y. Gao, B. Luo, H. Hu, F. Fan, G. Liu, L. Wang, *Nat. Commun.* **2020**, *11*, 2129.
[82] B. W. Veal, S. K. Kim, P. Zapol, H. Iddir, P. M. Baldo, J. A. Eastman, *Nat. Commun.* **2016**, *7*, 11892.
[83] A. Kahn, *Mater. Horiz.* **2015**, *3*, 7.
[84] M. T. Greiner, L. Chai, M. G. Helander, W. M. Tang, Z. H. Lu, *Adv. Funct. Mater.* **2012**, *22*, 4557.
[85] Y. Zhang, Y. Li, X. Xin, Y. Wang, P. Guo, R. Wang, B. Wang, W. Huang, A. J. Sobrido, X. Li, *Nat. Energy* **2023**, *8*, 504.
[86] S. Sun, R. Gao, X. Liu, L. Pan, C. Shi, Z. Jiang, X. Zhang, J. J. Zou, *Sci. Bull.* **2022**, *67*, 389.
[87] R. Chen, S. Pang, H. An, J. Zhu, S. Ye, Y. Gao, F. Fan, C. Li, *Nat. Energy* **2018**, *3*, 655.
[88] F. Xu, K. Meng, S. Cao, C. Jiang, T. Chen, J. Xu, J. Yu, *ACS Catal.* **2021**, *12*, 164.
[89] Z. Wei, W. Wang, W. Li, X. Bai, J. Zhao, E. C. M. Tse, D. L. Phillips, Y. Zhu, *Angew. Chem., Int. Ed.* **2021**, *60*, 8236.
[90] J. Wang, Z. Wang, J. Zhang, S.-P. Chai, K. Dai, J. Low, *Nanoscale* **2022**, *14*, 18087.
[91] Y. Zhou, Z. Zhang, Z. Fang, M. Qiu, L. Ling, J. Long, L. Chen, Y. Tong, W. Su, Y. Zhang, J. C. S. Wu, J. M. Basset, X. Wang, G. Yu, *Proc. Natl. Acad. Sci. U.S.A.* **2019**, *116*, 10232.
[92] Y. Chao, P. Zhou, N. Li, J. Lai, Y. Yang, Y. Zhang, Y. Tang, W. Yang, Y. Du, D. Su, Y. Tan, S. Guo, *Adv. Mater.* **2019**, *31*, 1807226.
[93] J. Zhao, S. Xue, R. Ji, B. Li, J. Li, *Chem. Soc. Rev.* **2021**, *50*, 12070.
[94] D. Y. Wan, Y. L. Zhao, Y. Cai, T. C. Asmara, Z. Huang, J. Q. Chen, J. Hong, S. M. Yin, C. T. Nelson, M. R. Motapothula, B. X. Yan, D. Xiang, X. Chi, H. Zheng, W. Chen, R. Xu, Ariando, A. R., A. M. Minor, M. B. H. Breese, M. Sherburne, M. Asta, Q. H. Xu, T. Venkatesan, *Nat. Commun.* **2017**, *8*, 15070.
[95] C. F. Tan, A. K. Su Su Zin, Z. Chen, C. H. Liow, H. T. Phan, H. R. Tan, Q. H. Xu, G. W. Ho, *ACS Nano* **2018**, *12*, 4512.
[96] L. Zhou, Z. Liu, Z. Guan, B. Tian, L. Wang, Y. Zhou, Y. Zhou, J. Lei, J. Zhang, Y. Liu, *Appl. Catal. B. Environ.* **2020**, *263*, 118326.
[97] X. Li, D. Wang, Y. Zhang, L. Liu, W. Wang, *Nano Res.* **2020**, *13*, 3025.
[98] G. Prusty, J. T. Lee, S. Seifert, B. B. Muhoberac, R. Sardar, *J. Am. Chem. Soc.* **2020**, *142*, 5938.
[99] E. L. Runnerstrom, A. Bergerud, A. Agrawal, R. W. Johns, C. J. Dahlman, A. Singh, S. M. Selbach, D. J. Milliron, *Nano Lett.* **2016**, *16*, 3390.
[100] Y. Lu, X. Jia, Z. Ma, Y. Li, S. Yue, X. Liu, J. Zhang, *Adv. Funct. Mater.* **2022**, *32*, 2203638.
[101] D. Mateo, J. L. Cerrillo, S. Durini, J. Gascon, *Chem. Soc. Rev.* **2021**, *50*, 2173.
[102] S. Fang, Y. H. Hu, *Chem. Soc. Rev.* **2022**, *51*, 3609.
[103] W. Gao, Y. Li, D. Xiao, D. Ma, *J. Energy Chem.* **2023**, *83*, 62.
[104] M. Cai, Z. Wu, Z. Li, L. Wang, W. Sun, A. A. Tountas, C. Li, S. Wang, K. Feng, A.-B. Xu, S. Tang, A. Tavasoli, M. Peng, W. Liu, A. S. Helmy, L. He, G. A. Ozin, X. Zhang, *Nat. Energy* **2021**, *6*, 807.
[105] D. Liu, Y. Xu, M. Sun, Y. Huang, Y. Yu, B. Zhang, *J. Mater. Chem. A.* **2020**, *8*, 1077.
[106] M. Gao, C. K. Peh, L. Zhu, G. Yilmaz, G. W. Ho, *Adv. Energy Mater.* **2020**, *10*, 2000925.
[107] a) Y. Qi, L. Song, S. Ouyang, X. Liang, S. Ning, Q. Zhang, J. Ye, *Adv. Mater.* **2020**, *32*, 1903915; b) Y. Cheng, Y. Chang, Y. Feng, H. Jian, Z. Tang, H. Zhang, *Angew. Chem., Int. Ed.* **2018**, *57*, 246.
[108] M. Wang, K. Deng, W. Lu, X. Deng, K. Li, Y. Shi, B. Ding, Z. Cheng, B. Xing, G. Han, Z. Hou, J. Lin, *Adv. Mater.* **2018**, *30*, 1706747.
[109] Y. Tang, W. Zhou, Q. Shang, Y. Guo, H. Hu, Z. Li, Y. Zhang, L. Liu, H. Wang, X. Tan, *Appl. Catal. B. Environ.* **2022**, *310*, 121295.
[110] S. Luo, H. Lin, Q. Wang, X. Ren, D. Hernandez-Pinilla, T. Nagao, Y. Xie, G. Yang, S. Li, H. Song, M. Oshikiri, J. Ye, *J. Am. Chem. Soc.* **2021**, *143*, 12145.
[111] Z. Chen, Q. Zhang, Y. Luo, *Angew. Chem., Int. Ed.* **2018**, *57*, 5320.
[112] J. Low, B. Dai, T. Tong, C. Jiang, J. Yu, *Adv. Mater.* **2019**, *31*, 1802981.
[113] C. Mu, C. Lv, X. Meng, J. Sun, Z. Tong, K. Huang, *Adv. Mater. Interfaces* **2022**, *10*, 2201842.
[114] L. Pan, M. Ai, C. Huang, L. Yin, X. Liu, R. Zhang, S. Wang, Z. Jiang, X. Zhang, J. J. Zou, W. Mi, *Nat. Commun.* **2020**, *11*, 418.
[115] W. Gao, R. Peng, Y. Yang, X. Zhao, C. Cui, X. Su, W. Qin, Y. Dai, Y. Ma, H. Liu, Y. Sang, *ACS Energy Lett.* **2021**, *6*, 2129.

Di Zu received her Ph.D. degree from the Department of Physics at Tsinghua University, Beijing, China, in 2020. She is currently a Post-doctoral Fellow in the Department of Applied Physics at The Hong Kong Polytechnic University. Her main research interests include the design of nanostructured photocatalysts for energy and environmental applications, defects engineering, and photothermal materials.

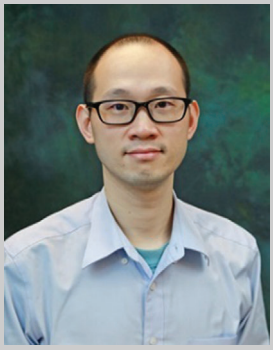

Yuen Hong Tsang received his B.Sc. and Ph.D. degrees in Physics from the University of Manchester, UK, in 2000 and 2004, respectively. He is currently working as a Professor in the Department of Applied Physics at The Hong Kong Polytechnic University. Dr. Tsang's academic research interests cover topics including novel 2D materials and nanostructure used for optics and photonic devices, laser materials, high-power lasers, and novel materials for energy applications.

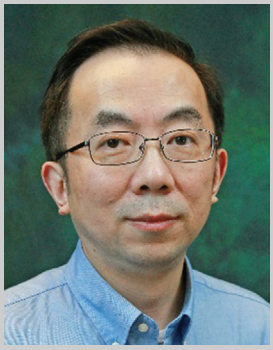

Haitao Huang received his B.Sc. in Physics from Shanghai Jiao Tong University and his Ph.D. in Materials Science from Nanyang Technological University. He is currently a professor in the Department of Applied Physics at Hong Kong Polytechnic University. His research interests include nanostructured materials for energy storage and conversion, and ferroelectric materials for energy applications. He is a Fellow of the Royal Society of Chemistry (RSC) and a board committee member of the International Academy of Electrochemical Energy Science (IAOEES).